Comparison of compositional MRI techniques to quantify the regenerative potential of articular cartilage: a preclinical minipig model after osteochondral defect treatments with autologous mesenchymal stromal cells and unseeded scaffolds

Karl Ludger Radke[1], Vera Grotheer[2]^, Benedikt Kamp[1], Anja Müller-Lutz[1], Justus Kertscher[1], Rosanna Strunk[1], Petros Martirosian[3], Birte Valentin[1], Hans-Jörg Wittsack[1], Martin Sager[4], Joachim Windolf[2], Gerald Antoch[1], Erik Schiffner[2], Pascal Jungbluth[2], Miriam Frenken[1]

[1]Department of Diagnostic and Interventional Radiology, Faculty of Medicine, University Hospital Düsseldorf, Düsseldorf, Germany; [2]Department of Orthopedics and Trauma Surgery, Heinrich Heine University Hospital Düsseldorf, Düsseldorf, Germany; [3]Department of Diagnostic and Interventional Radiology, Faculty of Medicine, University Hospital Tübingen, Tübingen, Germany; [4]Central Unit for Animal Research and Animal Welfare Affairs, University Hospital, Heinrich Heine University, Düsseldorf, Germany

Contributions: (I) Conception and design: KL Radke, V Grotheer, B Kamp, M Sager, E Schiffner, P Jungbluth, M Frenken; (II) Administrative support: KL Radke, V Grotheer, A Müller-Lutz, HJ Wittsack, E Schiffner, P Jungbluth, M Frenken; (III) Provision of study materials or patients: P Martirosian, M Sager, J Windolf, G Antoch; (IV) Collection and assembly of data: KL Radke, B Kamp, J Kertscher, R Strunk, B Valentin; (V) Data analysis and interpretation: KL Radke, E Schiffner, P Jungbluth, M Frenken; (VI) Manuscript writing: All authors; (VII) Final approval of manuscript: All authors.

Correspondence to: Vera Grotheer, PD Dr. Department of Orthopedics and Trauma Surgery, Heinrich Heine University Hospital Düsseldorf, Moorenstr. 5, 40225 Düsseldorf, Germany. Email: vera.grotheer@med.uni-duesseldorf.de.

Background: The field of orthopedics seeks effective, safer methods for evaluating articular cartilage regeneration. Despite various treatment innovations, non-invasive, contrast-free full quantitative assessments of hyaline articular cartilage's regenerative potential using compositional magnetic resonance (MR) sequences remain challenging. In this context, our aim was to investigate the effectiveness of different MR sequences for quantitative assessment of cartilage and to compare them with the current gold standard delayed gadolinium-enhanced MR imaging of cartilage (dGEMRIC) measurements.

Methods: We employed *ex vivo* imaging in a preclinical minipig model to assess knee cartilage regeneration. Standardized osteochondral defects were drilled in the proximal femur of the specimens (n=14), which were divided into four groups. Porcine collagen scaffolds seeded with autologous adipose-derived stromal cells (ASC), autologous bone marrow stromal cells (BMSC), and unseeded scaffolds (US) were implanted in femoral defects. Furthermore, there was a defect group which received no treatment. After 6 months, the specimens were examined using different compositional MR methods, including the gold standard dGEMRIC as well as T_1, T_2, T_2^*, and $T_{1\rho}$ techniques. The statistical evaluation involved comparing the defect region with the uninjured tibia and femur cartilage layers and all measurements were performed on a clinical 3T MR Scanner.

Results: In the untreated defect group, we observed significant differences in the defect region, with dGEMRIC values significantly lower (404.86±64.2 ms, P=0.018) and T_2 times significantly higher (44.24±2.75 ms, P<0.001). Contrastingly, in all three treatment groups (ASC, BMSC, US), there were no significant differences among the three regions in the dGEMRIC sequence, suggesting successful cartilage

^ ORCID: 0000-0001-6034-9608.

regeneration. However, T_1, $T_2{}^*$, and $T_{1\rho}$ sequences failed to detect such differences, highlighting their lower sensitivity for cartilage regeneration.

Conclusions: As expected, dGEMRIC is well suited for monitoring cartilage regeneration. Interestingly, T_2 imaging also proved to be a reliable cartilage imaging technique and thus offers a contrast agent-free alternative to the former gold standard for subsequent *in vivo* studies investigating the cartilage regeneration potential of different treatment modalities.

Keywords: Cartilage regeneration therapy; compositional magnetic resonance imaging (MRI); adipose-derived stromal cells (ASC); bone marrow-derived mesenchymal stromal cells (BMSC)

Introduction

Osteoarthritis (OA) is a common musculoskeletal disorder, and its prevalence is expected to increase due to the aging population and endemic obesity with a prevalence in Europe & the United States (1,2). One of the characteristic features of OA is irreversible cartilage degradation and subsequent pathological changes in the surrounding tissues (3,4). As a result, surgical interventions such as implantation of cartilage substitutes like collagen scaffolds seeded with adipose-derived stromal cells (ASC), bone marrow stromal cells (BMSC), or unseeded scaffolds (US) have become increasingly relevant. They have been investigated in several studies (5-7). Nevertheless, there is an apparent deficiency in methodically consistent studies that rigorously assess the capability of these varied treatment modalities to regenerate cartilage. Magnetic resonance imaging (MRI) has the potential to offer invaluable insights into the composition and structure of cartilage, extending beyond mere morphological analysis. Hence, employing advanced MRI techniques for a detailed quantitative evaluation presents an enticing prospect to significantly enhance our comprehension of cartilage regeneration therapies and gauge their efficacy.

In previous studies, compositional magnetic resonance (MR) sequences that allow characterization of the biochemical composition, such as delayed gadolinium-enhanced MRI of cartilage (dGEMRIC), T_1, $T_{1\rho}$, T_2, and $T_2{}^*$ mapping have shown an excellent ability to detect the quantitative morphological changes in cartilage (4,8-11). Compared to morphological sequences like T_2-weighted (T_{2w}) or proton density-weighted (PD) sequences, compositional MR sequences provide more detailed information about the structure and composition

of cartilage tissue (10). Moreover, compared to other biosensitive sequences such as chemical exchange saturation transfer (CEST) (12,13), quantitative susceptibility mapping (QSM) (14), and ^{23}Na (15) imaging, the MRI techniques do not require specific hardware, are less susceptible to noise, require simpler post-processing, and are more commonly used and validated, making them suitable for our focus on more straightforward clinical translation.

Using OA as an example, the importance of compositional MRI techniques can be noted. In the early stages of OA, the cartilage microstructure breaks down and the tissue begins to lose its functional capacity. These changes occur before morphologic cartilage changes, which occur at an advanced stage of OA and can be visualized by compositional MRI. Thus, these novel techniques provide measurements that correlate with various physiological properties of cartilage and can detect disease earlier than conventional imaging techniques (10,16).

In order to characterize cartilage as accurately as possible, a combination of several quantitative MRI techniques is required (17). Articular cartilage consists of approximately 70–80% fluid and 20–30% solid extracellular matrix (ECM) (18). The ECM consists of a network of highly organized collagen fibrils and proteoglycan (PG) molecules (19). Among these techniques, dGEMRIC, employs a negatively charged contrast agent to facilitate the indirect measurement of the fixed charge density of glycosaminoglycans (GAGs) within the cartilage (20,21). dGEMRIC, a contrast-enhanced technique, has been shown in several studies to be a sensitive method for imaging cartilage composition and is therefore considered as gold standard. Currently contrast agent-free techniques are being investigated, such as $T_{1\rho}$ imaging, which allows the

investigation of proton motion by relaxation measurement in the rotating frame induced by an additional radiofrequency (RF) pulse (22). This can provide information about the stiffness and integrity of the cartilage tissue and has a dependence on PG concentration (23,24). In contrast, MR sequences such as T_1 and T_2 measure the relaxation times of protons in the tissue and provide information about the water content and density of cartilage (25,26). Furthermore, T_2^* relaxation time is mainly influenced by collagen alignment and thus reflects the biochemical composition of cartilage (27,28).

Most previous studies on the regenerative potential of cartilage have focused on *in vitro* analysis (29-31). To bridge the gap between *in vitro* experiments and *in vivo* applications in humans, our study used an appropriate minipig model to assess the chondral regeneration potential of three different treatment options: autologous ASC, autologous BMSC treated scaffolds and US, our primary objective was to investigate the capabilities of MR compositional analysis in representing this cartilage regeneration. The minipig model was used for evaluating osteochondral regeneration due to its comparable joint size to humans, similar weight-bearing and gait characteristics, and similar physiology of cartilage regeneration (32). Our hypothesis was that this multiparametric assessment would provide a comprehensive MR evaluation of cartilage regeneration potential and reveal differences in sensitivity between MR methods, allowing reduced sequence selection for subsequent *in vivo* studies. This approach allows a more thorough investigation of the potential for cartilage regeneration compared to conventional *in vitro* experiments and provides valuable insights for future clinical implementation. We represent this article in accordance with the ARRIVE reporting checklist (available at https://qims.amegroups.com/article/view/10.21037/qims-23-570/rc).

Methods

Study design

This study was designed as a prospective, comparative and randomized preclinical MR imaging study in which experiments were performed in accordance with the institutional guidelines for the care and use of laboratory animals at the Heinrich Heine University, Medical Faculty. The study was approved by the regional authority: Landesamt für Natur-, Umwelt- und Verbraucherschutz, LANUV NRW, Germany under application number: 81-

02.04.2020.A198. For this, a case count planning was performed by the statistical advice of the medical faculty of the Heinrich Heine University to ensure sufficient power to detect statistically significant differences while minimizing the number of animals used.

In total 14 Aachener minipigs derived from Hanford pigs and the Columbian potbellied pig, were bred in the animal testing facility of Düsseldorf (The Central Institution for Animal Research and Scientific Animal Protection; ZETT). Of these seven male and seven female, aged (Ø=4.4 years), with an average weight (Ø=112,25 kg) were surgically dissected on both hind legs (28 knee specimens). And randomly distributed among four groups, with seven knees each, in which they were either treated with autologous ASC, autologous BMSC, US or did not receive any therapy (defect group). For randomization, the pigs were divided in a female and a male block and then by flipping a coin classified in the control and treatment group (head: control, tail: treatment). In the stables were light from 7 am to 7 pm. The temperature was 21 ℃ and the humidity was between 55% and 65%. The food was from the Sniff company, Minipig maintenance, Energy reduced, 4 mm. Inclusion criteria for study participation were (I) perfect health condition, (II) same origin, (III) approximately the same weight and age. Two minipigs had to be excluded due to an infection and a neurological problem before the investigation of the effectiveness of different MR sequences. The animals were allowed to move freely for a period of six months, after which they were euthanized and evaluated using compositional MR methods. A careful optimization process was carried out for the MR sequences. For this purpose, two knees were fine-tuned in detail under variation of the essential parameters such as repetition time (TR), echo time (TE), and field of view (FOV) with regard to optimization of the image quality. The preparation for the dGEMRIC measurement was also optimized. In order to maintain the consistency of the data and to avoid subject-specific bias of the individual methods, the two knee samples used in the optimization process were excluded from the remaining data set. Subsequently, the MRI examination results were compared, and the sensitivity of the various MRI sequences was evaluated based on their ability to reveal significant differences between the different regions.

Surgical procedure and treatment methods

All surgical procedures were performed by the same team,

7470

Radke et al. Evaluating MRI techniques in cartilage regeneration

Figure 1 Intraoperative picture of defect preparation. The chondral defects were created at the limb (*), with a hollow cutter ($) in the central area of the medial femoral condyle (π) and Langenbeck retractors (ρ) were used to restrain the tissue.

including two orthopaedic surgeons (with 19 and 12 years of experience), one anaesthetist (with 30 years of experience) and one laboratory technician (with 30 years of experience) in charge of isolating cells. First peripheral venous access was established. In order to be able to intubate the pig, it must first be placed under sufficiently deep anesthesia. For this purpose, a short-term barbiturate was injected i.v. (thiopental 8–15 mg/kg). If the muscle tension of the jaw ceased, the animal would be intubated. Subsequently, both the animal and the surgical field were prepared. The animal was then taken to the operating room, bandaged, and inhalation anesthesia was induced (Isofluran 1.0–2.0 Vol.% + O_2-room air mixture), maintained (Isofluran 1.3% + O_2-room air mixture) and the respective leg was disinfected. Thirty minutes before the surgery started Piritramid (0.3 mg/kg) was i.v. injected. The reflexes were checked. After that, the surgery was started. A medial parapatellar approach was used in all procedures. After the medial condyle was exposed, we always placed the hollow cutter at the center of the condyle, perpendicular to the chondral surface and with the same axis as the femoral shaft so that all of the defects were at the same location (*Figure 1*). According to the defect models published by Betsch *et al.* and Gotterbarm *et al.* a chondral defect of 6.3 mm

diameter was created (33,34). To prevent haemorrhage, the manipulation was carried out carefully in order to not penetrate the subchondral bone. The operating field was irrigated with physiological saline during the process to wash off the chondral debris and prevent dehydration of the cartilage. Intraoperative analgesia was provided every 30 minutes i.v. with fentanyl (0.01–0.03 mg/kg). At the end of the surgery, therapy was initially started with initial meloxicam (0.4 mg/kg). The postoperative analgesia was orally continued until day 10 with meloxicam (0.2 mg/kg). Wound closure was accomplished with bioresorbable sutures and the animals were then returned to their enclosure and monitored until full recovery.

The treatment of the total of 28 defects was divided into four treatment groups: (I) empty (defect group) (7 defects), (II) OptiMaix 3D® (Matricel GmbH, Herzogenrath, Germany) as a US (7 defects), (III) BMSC + OptiMaix 3D® scaffold (7 defects) and (IV) adipose stromal cells (ASC) + OptiMaix 3D® scaffold (US) (7 defects). The Optimaix-3D scaffold is an open-porous porcine collagen I/III sponge (<30% w/w elastin) with a porosity of 98% and pore sizes around 85 μm, as described in Möllers *et al.* (35). The size of the scaffold was 6.3 mm in diameter and 1.5 mm in height. The scaffold was carefully placed into the defect site using gentle pressure to ensure secure placement and optimal contact with the surrounding tissue.

The pigs that underwent mesenchymal stromal cell therapy received a 2-stage procedure. In the first step, BMSCs were harvested from the iliac crests by Jamshidi vacuum aspiration. In this procedure, ASC was harvested from *subcutaneous hip adipose tissue*. As published before BMSC and ASC were isolated as described previously and then cultivated in Dulbecco's Modified Eagle Medium (DMEM) (4.5 g/L glucose) supplemented with 2 mM α-glutamine (PPA Laboratories, Cölbe, Germany), 100 U/mL penicillin (Sigma-Aldrich, Taufkirchen, Germany), 100 μg/mL streptomycin (PPA Laboratories) and 10% fetal bovine serum (FBS) at 37 ℃ in a humidified atmosphere, containing 5% CO_2. If necessary, cells were frozen in N_2. Before reimplantation ASC and BMSC were chondrogenically differentiated for 5 days with 1% insulin-transferrin-selenium (Sigma-Aldrich), 10 ng/mL TGF-β1 (Pepro Tech, Hamburg, Germany) and 1 μg/mL α-Ascorbin-2-Phosphat (Sigma-Aldrich). Afterward, cells were washed two times with phosphate-buffered saline (PBS; Sigma-Aldrich) and then applied on the scaffold in a cell density of 1×10^7 for 20–30 minutes before reimplantation according to the published approach of Jurgens *et al.* (36). In
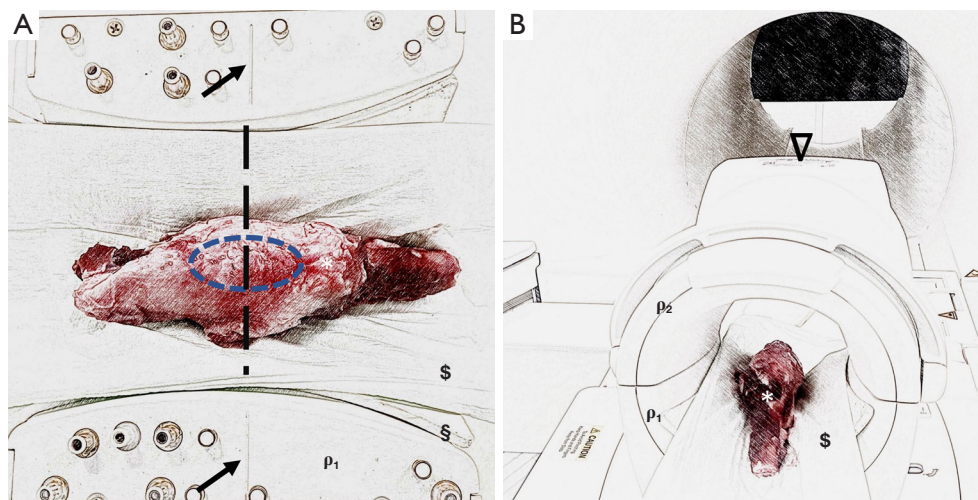
Figure 2 Experimental setup to investigate chondral regeneration potential using biosensitive MR sequences on an established minipig model. (A) Knee specimens (*) were placed in the supine position, feet first, in a clinical knee coil (ρ_1, which is open for better illustration) and fixed with mechanical positioning aids such as pads (§) and cloths ($). Marker lines (black arrows) located on the coil were used for standardized specimen placement. Here, the knee joint (blue ellipse) was placed centrally in the coil. (B) Once the knee sample was centrally positioned in the knee coil, the coil was closed (ρ_1 and ρ_2) and then positioned centrally in the MRI using the reference markings on the top (▽) of the coil.

the second step after a 12-week recovery period the group underwent the surgical procedure. The defect in three knee groups was filled with OptiMaix 3D®. Prior implantation BMSC and ASC were added to the scaffolds.

After 6 months the animals from all groups were euthanized and both back limbs were retrieved by exarticulation at the hip joint. Then, the femur and tibia bones were sectioned proximal and distal to the knee joint, with all peripheral soft tissue for the following MRI measurements.

MR image acquisition

Each sectioned knee joint specimen was measured individually in the supine position, feet first, and examined by MRI. For this purpose, a clinical 3.0 T MRI scanner (MAGNETOM Trio, Siemens Healthineers, Erlangen, Germany) and an 8-channel knee coil (8 CHANNEL KNEE COIL, Siemens Healthineers) were used. Mechanical positioning devices such as cloths and pads were used to hold the knee specimen in place during the MRI scan. The kneecap was centrally aligned using the guidelines provided on the coil (Figure 2).

The MR protocol included both a morphologic sequence and compositional measurements. Specifically, a high-resolution double-echo steady-state (DESS) sequence, gradient-echo T_2^* mapping sequence, T_2 mapping sequence, $T_{1\rho}$ sequence, and double-flip-angle T_1 mapping sequence were performed (Table 1). The T_1 sequence was executed both without contrast agent (T_1) and with a contrast agent (dGEMRIC). These were carried out after the initial positioning of the knee within the MRI scanner. To acquire the dGEMRIC measurements, the knee joint specimen was removed from the scanner. Subsequently, the anterior knee capsule was surgically incised using a fine scalpel, without affecting the cartilage integrity, and stored for 60 minutes in a vessel containing a gadolinium MR contrast agent used in routine clinical practice (Clariscan, GE Healthcare Buchler GmbH, Braunschweig, Germany) diluted to a concentration of 2.5 mmol/L with clinical NaCl (Fresenius Kabi Deutschland GmbH, Bad Homburg, Germany) (37,38). Following this, the knee specimen was repositioned in the MRI scanner, consistent with the earlier measurements, and the T_1 mapping as dGEMRIC was recorded again, along with another DESS to ensure consistency between measurements at both time points. All MRI measurements were performed at room temperature. The knee specimens were warmed to room temperature for 48 hours prior to measurement. The magnetization time per sample was approximately 1.25 hours, and the examination time was 2.25 hours.

Table 1 Detailed sequence parameters of the morphological and biosensitive sequences

Sequence parameters	Morphological	Biosensitive			
		T_2^*	T_2	$T_{1\rho}$	$T_{1/dGEMRIC}$
Sequence type	DESS	GRE	SE	TFL magnprep	VIBE
Orientation	Cor	Cor	Cor	Cor	Cor
TR, ms	14.69	38	4,000	3,500	15
TE, ms	4.42	4.92, 9.84, 14.76, 19.68, 24.60, 29.52	11.7, 23.4, 35.1, 46.8, 58.5, 70.2, 81.9, 93.6, 105.3, 117	5.33	2.22
Average	1	1	1	1	1
Field of view, mm × mm	160×160	160×160	160×160	160×160	160×160
Acquisition matrix, pixels	512×512	256×256	256×256	192×192	256×256
Flip angle, °	25	25	180	15	5 and 26
Slices	256	176	30	64	176
Pixel size, mm × mm	0.31×0.31	0.63×0.63	0.63×0.63	0.80×0.80	0.63×0.63
Slice thickness, mm	0.31	0.63	1.2	1.2	0.63
Spin lock duration, ms	NA	NA	NA	0, 20, 80, 140	NA
Duration, min	8:30	8:58	9:26	16:25	12:21

DESS, double-echo steady-state; dGEMRIC, delayed gadolinium-enhanced magnetic resonance imaging of cartilage; GRE, gradient echo; SE, spin echo; TFL magnprep, Turbo Flash magnetic preparation; VIBE, volumetric interpolated breath-hold examination; Cor, coronal; TR, repetition time; TE, echo time; NA, not available.

Post-processing

Knee specimens were manually segmented using the brush and polygon tools of ITK-SNAP software (v3.8.0, Cognitica, Philadelphia, PA, USA) by a clinical radiologist with seven years of musculoskeletal imaging experience blinded to the animal treatment. Manual segmentation of the knee specimens included the femoral cartilage layer, tibial cartilage layer, and the region of the standardized defect on the medial femoral condyle. All segmentations were performed on the two high-resolution DESS sequences, taking care to exclude marginal voxels at the joint-fluid interface to reduce partial volume effects. Based on the spatial information stored in the DICOM header, the DESS masks were transformed to the biosensitive MR sequences using a custom Python framework (Github: https://github.com/MPR-UKD/MaskRegistration). The script we developed for this purpose has a graphical interface and is made freely available for subsequent studies via the GNU license.

Subsequently, the relaxation times T_2^*, T_2, and $T_{1\rho}$ were determined voxel-wise using exponentially fitting routines (Eqs. [1-3]) to obtain information about the properties of the cartilage tissue to infer its composition and structure. Compositional evaluations were performed using a Python framework that we developed, and that is freely available under the GNU license (GitHub: https://github.com/MPR-UKD/bMRI). We used the Levenberg-Marquardt algorithm, an iterative method based on minimizing the squared error between the raw data and the calculated data.

$$T_2^*\text{-Fitting: } S(TE) = S_0 \exp\left(-\frac{t}{T2*}\right) + const \qquad [1]$$

$$T_2\text{-Fitting: } S(TE) = S_0 \exp\left(-\frac{t}{T2}\right) + const \qquad [2]$$

$T_{1\rho}$-Fitting:

$$S(TSL) = S_0 \sin(\alpha)\frac{\exp\left(-\frac{TSL}{T1\rho}\right)\left(1-\exp\left(-\frac{TR-TSL}{T1}\right)\right)\exp\left(-\frac{TE}{T2*}\right)}{1-\exp\left(-\frac{TSL}{T1\rho}\right)\exp\left(-\frac{TR-TSL}{T1}\right)\cos(\alpha)} + const \qquad [3]$$

The T_1 and $T_{1,dGEMRIC}$ relaxation maps were automatically calculated using two different flip angles on the scanner and evaluated using the transferred masks.

Statistical analysis

Statistical analyses were performed by KLR in R (v4.1.3, R Foundation for Statistical Computing). In this study, our aim was to track the regeneration potential of knee cartilage within individual subjects rather than comparing across groups. Therefore, each group was assessed separately with a Friedman test. Individual regions, i.e., femoral, tibial and lesion areas, were compared for each subject as the main aim of our statistical analysis was to determine whether the expected intra-subject changes could be represented by compositional MRI methods. A post hoc Wilcoxon signed rank test was used to detect significant differences between the regions, given that these are inherently paired measurements within the same knee joint. Due to the experimental design of this study, the significance level in the post hoc tests and multiple comparisons of the individual relaxation times was corrected using Bonferroni's conservative alpha adjustment method to prevent inflation of the alpha error. An adjusted significance level of $P \leq 0.05$ was used in all statistical analyses.

Results

Laboratory animals

The study included 14 experimental animals (28 knee specimens), of which 26 were investigated by compositional MR. Two knees were used for sequence optimization. Among the remaining 26 knee specimens, seven were treated with scaffolds that had been seeded with ASC, five with BMSC, seven were administered US, and seven served as the defect group, receiving no treatment.

Compositional analyses

We observed different levels of precision in the validation of cartilage quality when analyzing the different compositional MR sequences (*Table 2*).

dGEMRIC

Significant differences were observed in the defect group, between the defect region and the uninjured cartilage layer of tibia and femur, with the defect region exhibiting the lowest values at 404.86±64.2 ms (*Figure 3*), as determined by a Friedman test, with a P value of 0.018. In contrast, no statistically significant differences were detected in the dGEMRIC sequence among the three regions studied, i.e., tibia, femur, and defect, for all three groups that

received therapy: ASC (P=0.368), BMSC (P=0.074), and US (P=0.565).

T_1

A significant increase in T_1 values was observed in the defect region for the US group (P=0.021), as determined by a Friedman test and confirmed in post-hoc tests. For the BMSC group, we observed significant differences (P=0.022), but this was not confirmed by post-hoc tests. In contrast, no statistically significant variations were detected in T_1 values without contrast agent among the three regions studied, i.e., tibial, femoral, and defect, for ASC (P=0.317) and defect (P=0.495) groups (*Figure 4*).

$\Delta T1$

In addition to the dGEMRIC and T_1 evaluation, we determined the ΔT_1 ($T_1 - T_{1,dGEMRIC}$) values. Analogous to the dGEMRIC evaluation, we found significant (P=0.018) variations in the defect group only, as determined by a Friedman test. These variations were observed to be significant between the tibia and defect as well as between the femur and defect in post-hoc analyses (*Figure 5*), as determined by a Wilcoxon test.

T_2

Significant variations were observed in the T_2 sequence among the three regions studied in the ASC group (Friedman test, P=0.007), as determined by a Friedman test. Post-hoc analyses revealed significant differences between tibia and femur and between femur and defect, with the defect region having the lowest T_2 times of 39.42±4.47 ms. In contrast, although T_2 times were lower in the defect region than in the femur in both the BMSC and US groups, these differences were not statistically significant as determined by a post-hoc analysis. In the defect group, significant variations were observed between all regions (Friedman test, P<0.001), with the defect region having the highest T_2 times of 44.24±2.75 ms (*Figure 6*), as determined by a Friedman test.

T_2^*

Analogous to the T_1 evaluation, in our study we found significant variations between the three regions investigated only in the US group. In the US region, we observed significantly lower T_2^* values of 14.79±2.48 ms than in the tibia and femur regions as well as in the comparison regions of the other groups (*Figure 7*), as determined by a Friedman test with a P value of <0.001. In contrast, no

Table 2 Comparison of dGEMRIC, T_2, T_1, T_2^* and $T_{1\rho}$ values in the tibia, femur, and defect for the ASC, BMSC, defect and US groups

MRI techniques	Groups	Tibia	Femur	Defect
dGEMRIC, ms	ASC	521.36±119.08	484.85±161.14	461.70±175.88
	BMSC	533.46±77.51	443.23±105.52	432.03±170.03
	Defect	616.53±141.57	610.01±190.82	404.84±64.2
	US	599.00±227.09	647.55±237.60	649.81±295.73
T_2, ms	ASC	40.68±4.96	43.48±3.18	39.42±4.75
	BMSC	42.11±4.30	45.54±4.41	38.79±3.51
	Defect	36.71±2.15	40.92±4.36	44.24±2.75
	US	40.85±2.44	43.12±1.97	40.95±2.76
T_1, ms	ASC	901.62±103.67	839.15±38.97	857.51±102.81
	BMSC	930.69±134.36	847.16±107.18	925.47±106.36
	Defect	840.91±119.78	873.94±100.29	887.30±116.17
	US	875.45±69.8	899.64±63.83	1041.12±113.71
T_2^*, ms	ASC	17.18±4.21	18.14±3.26	17.28±3.32
	BMSC	17.95±4.44	18.65±2.62	15.21±2.79
	Defect	20.40±3.87	21.88±3.79	19.63±4.57
	US	18.75±2.39	21.52±2.73	14.79±2.48
$T_{1\rho}$, ms	ASC	75.57±8.01	88.85±9.80	83.15±9.19
	BMSC	78.65±7.23	98.54±7.85	75.61±13.07
	Defect	92.31±11.31	89.25±19.29	88.9±24.79
	US	82.54±14.52	91.06±7.28	94.65±11.61
ΔT_1, ms	ASC	380.26±145.64	354.30±174.50	395.81±230.61
	BMSC	397.22±164.95	403.93±76.61	493.44±203.46
	Defect	224.38±237.20	263.94±192.48	482.43±117.97
	US	276.46±192.06	252.08±223.23	391.32±381.68

Data are presented as mean ± standard deviation. dGEMRIC, delayed gadolinium-enhanced magnetic resonance imaging of cartilage; ASC, adipose-derived stromal cell; BMSC, bone marrow-derived mesenchymal stromal cell; US, unseeded scaffold; MRI, magnetic resonance imaging.

statistically significant variations were detected in the other groups, ASC (P=0.459), BMSC (P=0.074), and defect group (P=0.236).

T1ρ

In the BMSC we observed higher $T_{1\rho}$ values in the femur compared to the tibia, as determined by a Friedman test. In the defect group, the differences were similar, but they were not statistically significant as determined by a Friedman test. Additionally, in the ASC and US groups, the Friedman test did not yield any significant results in post-hoc analysis

(*Figure 8*).

Discussion

In this study, the regeneration potential of cartilage in the knee was evaluated using compositional MR imaging. The primary objective of this study was to evaluate and compare the sensitivity of different compositional MR sequences in their ability to visualize and assess changes related to cartilage regeneration following targeted defect placement. To this purpose, a preclinical feasibility study was conducted
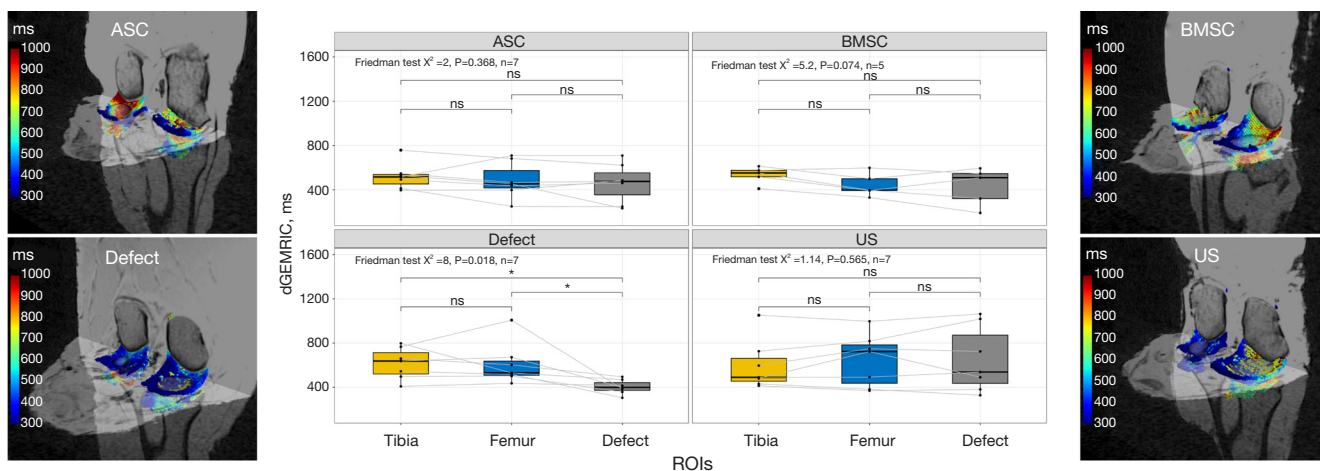
Figure 3 Boxplots and heat maps of dGEMRIC of cartilage relaxation times as a function of cartilage region and different treatment strategies: collagen scaffold seeded with ASC, seeded with BMSC, defect group without collagen scaffold, and US. The box indicates the IQR, with the median displayed as a line within the box. The whiskers extend up to 1.5 times the IQR, with any outliers depicted as individual points. *, P<0.05 was considered statistically significant. dGEMRIC, delayed gadolinium-enhanced magnetic resonance imaging of cartilage; ASC, adipose-derived stromal cell; BMSC, bone marrow-derived mesenchymal stromal cell; US, unseeded scaffold; ROI, region of interest; IQR, interquartile range.
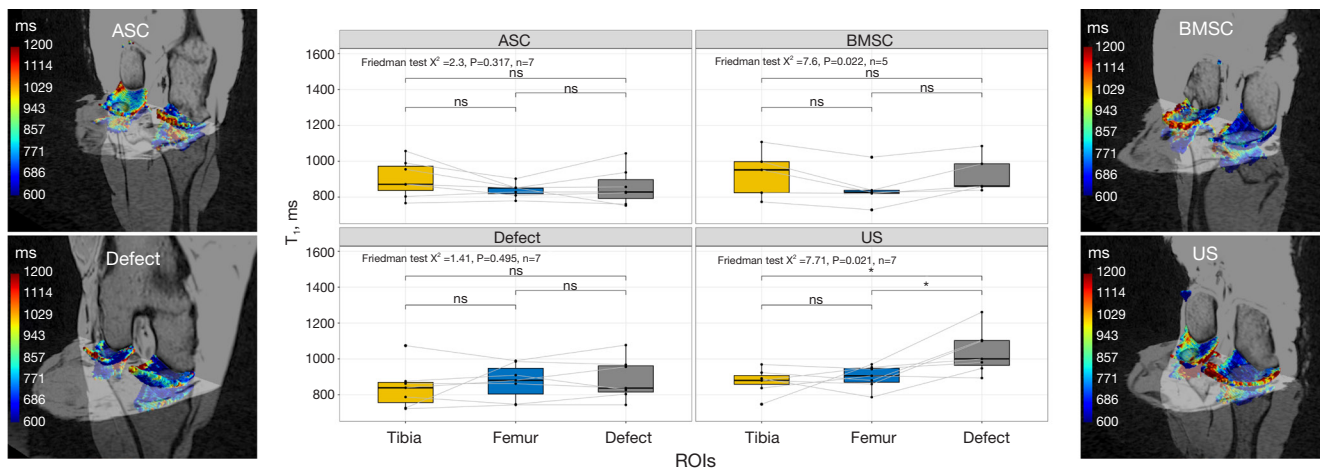
Figure 4 Visualization of T_1 relaxation times as Boxplot and 3D heat maps before contrast administration depending on cartilage region and different treatment strategies: collagen scaffold seeded with ASC, seeded with BMSC, defect group without collagen scaffold, and US. The box indicates the IQR, with the median displayed as a line within the box. The whiskers extend up to 1.5 times the IQR, with any outliers depicted as individual points. *, P<0.05 was considered statistically significant. ASC, adipose-derived stromal cell; BMSC, bone marrow-derived mesenchymal stromal cell; US, unseeded scaffold; ROI, region of interest; IQR, interquartile range.

using a standardized minipig model with compositional MR imaging. The main finding of the study was that compositional MR imaging, in particular the gold standard dGEMRIC, as well as ΔT_1 and T_2 imaging, are well-suited methods for monitoring cartilage regeneration potential. T_2 imaging is thus a contrast-free alternative to the

contrast agent-based dGEMRIC technique. Furthermore, we observed that regenerative cartilage therapies with populated (ASC, BMSC) and US significantly improve the regeneration potential compared to conservative treatment (defect group) in terms of biosensitive MR parameters.
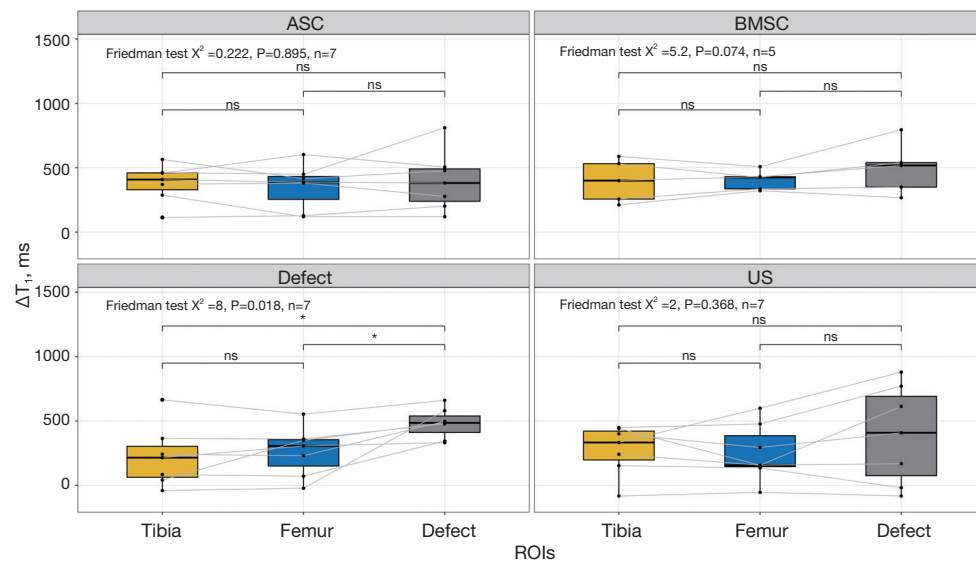
The first finding of the study is that dGEMRIC, the

7476

Radke et al. Evaluating MRI techniques in cartilage regeneration

Figure 5 Visualization of ΔT_1 relaxation times ($T_1 - T_{1,dGEMRIC}$) as Boxplot depending on cartilage region and different treatment strategies: collagen scaffold seeded with ASC, seeded with BMSC, defect group, and US. The box indicates the IQR, with the median displayed as a line within the box. The whiskers extend up to 1.5 times the IQR, with any outliers depicted as individual points. *, P<0.05 was considered statistically significant. dGEMRIC, delayed gadolinium-enhanced magnetic resonance imaging of cartilage; ASC, adipose-derived stromal cell; BMSC, bone marrow-derived mesenchymal stromal cell; US, unseeded scaffold; ROI, region of interest; IQR, interquartile range.
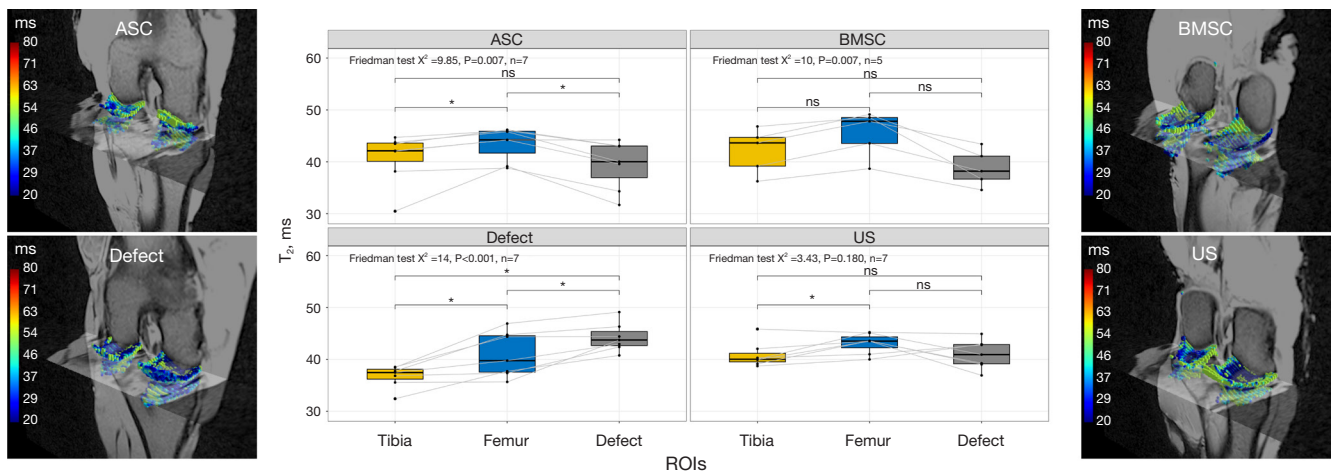
Figure 6 Visualization of T_2 relaxation times as Boxplot and 3D heat maps depending on cartilage region and different treatment strategies: collagen scaffold seeded with ASC, seeded with BMSC, defect group without collagen scaffold, and US. The box indicates the IQR, with the median displayed as a line within the box. The whiskers extend up to 1.5 times the IQR, with any outliers depicted as individual points. *, P<0.05 was considered statistically significant. ASC, adipose-derived stromal cell; BMSC, bone marrow-derived mesenchymal stromal cell; US, unseeded scaffold; ROI, region of interest; IQR, interquartile range.

gold standard of MR imaging, demonstrates a higher regeneration potential in injured cartilage that has been treated versus that which has remained untreated. In contrast to morphological MR imaging compositional

analyses allow a quantitative assessment of the regeneration potential of cartilage tissue. Currently, dGEMRIC imaging is considered the gold standard in compositional MR imaging. This method has been successfully validated
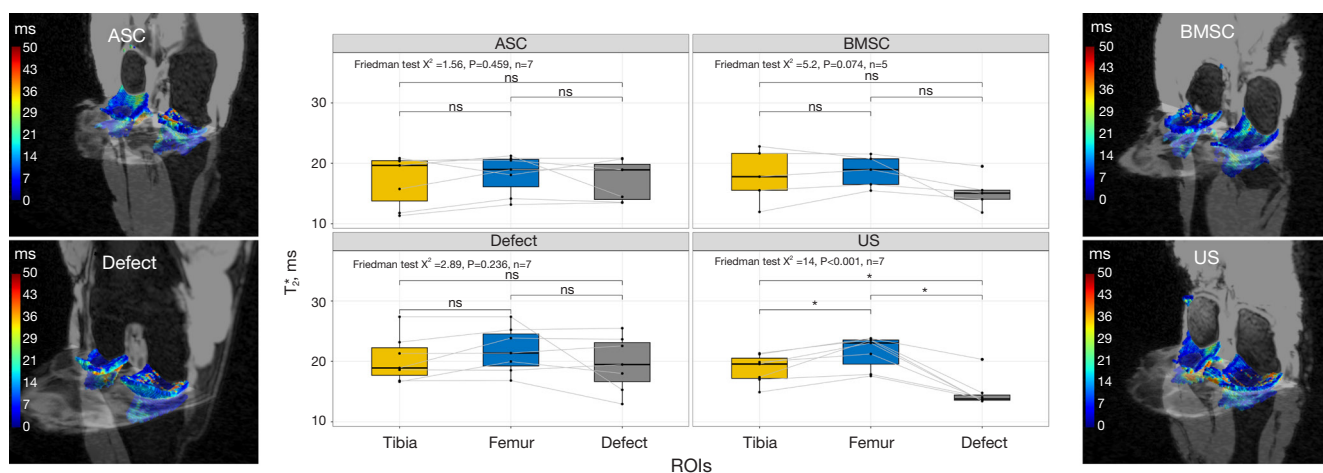
Figure 7 Visualization of T_2^* relaxation times as a function of cartilage region and different treatment strategies: collagen scaffold seeded with ASC, seeded with BMSC, defect group without collagen scaffold, and US. The box indicates the IQR, with the median displayed as a line within the box. The whiskers extend up to 1.5 times the IQR, with any outliers depicted as individual points. *, P<0.05 was considered statistically significant. ASC, adipose-derived stromal cell; BMSC, bone marrow-derived mesenchymal stromal cell; US, unseeded scaffold; ROI, region of interest; IQR, interquartile range.
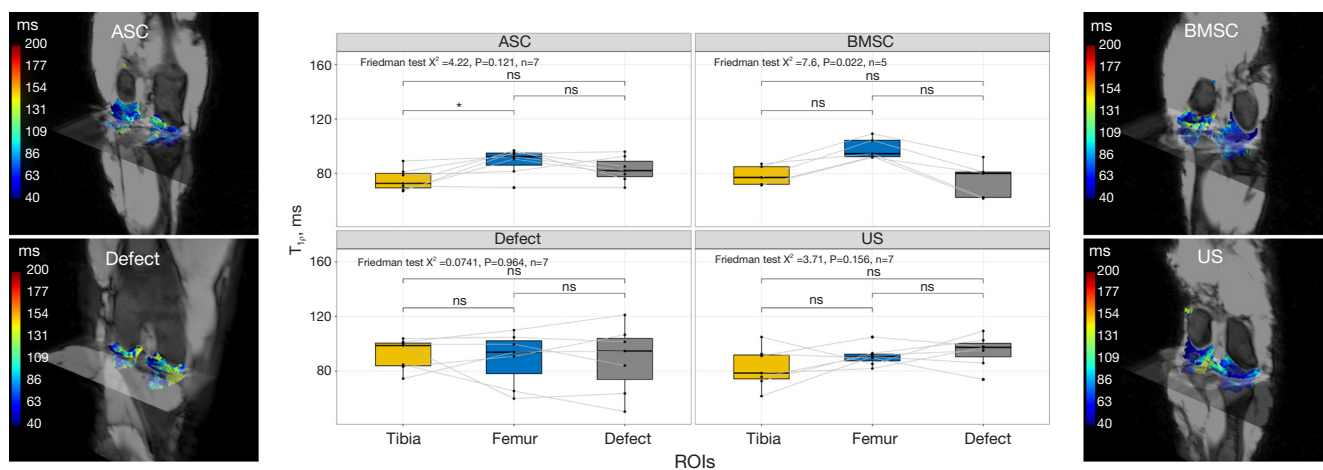

Figure 8 Visualization of $T_{1\rho}$ relaxation times as a function of cartilage region and different treatment strategies: collagen scaffold seeded with ASC, seeded with BMSC, defect group without collagen scaffold, and US. The box indicates the IQR, with the median displayed as a line within the box. The whiskers extend up to 1.5 times the IQR, with any outliers depicted as individual points. *, P<0.05 was considered statistically significant. ASC, adipose-derived stromal cell; BMSC, bone marrow-derived mesenchymal stromal cell; US, unseeded scaffold; ROI, region of interest; IQR, interquartile range.

in numerous *in vitro*, *ex vivo*, and *in vivo* studies and used in routine clinical practice (20,37,39,40). In our study, as expected, the defect group without therapy had lower dGEMRIC values, indicating a more advanced degeneration than all three treatment groups. Analogous to previous studies, we observed a significant decrease in measured dGEMRIC values after contrast administration in the defect group in the region of the defect, indicating a significant decrease in GAG concentration in this region (8,21,41). In contrast, the treatment groups (ASC, BMSC, US) showed no changes in dGEMRIC values compared to the femur and tibia regions, indicating regeneration of GAG and successful regeneration of cartilage in the treated regions.

The second finding of the study is that T_2 imaging is a useful, contrast-free alternative to dGEMRIC for evaluating cartilage regeneration in future *in vivo* studies. The T_2 imaging results showed significant differences between the defect area and the comparative regions in the knee within the untreated defect group. However, in the treated knees, there was a narrowing of the T_2 values of the cartilage defect area and the healthy comparative cartilage of the same knee. In the defect group, we observed an increase in T_2 values within the defect region, which may indicate an accumulation of free water such as synovial fluid. Synovial fluid has a longer T_2 time than cartilage so that partial volume effects may have occurred in our study region due to small progressive degeneration. This is also consistent with the observations of previous studies in which an increase in T_2 times was observed in OA patients (42,43).

Third, we also determined the T_1 times before contrast administration for dGEMRIC measurements. We found no significant differences between the femur cartilage and the cartilage defect region and the tibia cartilage and defect region in the defect group. Only in the US implant region a significant increase in T_1 times was observed. While dGEMRIC can mainly provide information about GAG concentration, T_1 time is mainly influenced by water concentration and cartilage density (25). The increase we observed in the US group suggests that the presence of a collagen scaffold alone is not sufficient to fully generate water content and density. In the groups treated with populated scaffolds (ASC and BMSC), we did not observe these effects, which may indicate that populating the scaffold with cells has a potentially positive effect on regeneration.

Fourth, the difference in T_1 relaxation times before and after contrast administration was evaluated with respect to the regeneration potential of knee cartilage. Because we determined the T_1 relaxation times both before and after contrast administration, we were able to determine the ΔT_1 times, i.e., which allows more accurate reproduction of the gadolinium-diethylenetriaminepentacetate (Gd-DTPA^{2-}) concentration in cartilage tissue (44). Here, the results of dGEMRIC imaging that we observed manifested themselves, where we consistently observed the largest differences between T_1 measurements before and after contrast in the defect area for all treatment strategies. However, this was significant only in the defect group. Nevertheless, for further *ex vivo* dGEMRIC studies, it is recommended that T_1 times be determined both before and after contrast injection, as this increases the sensitivity of

the technique and thus may allow significant discrimination of treatment methods in larger groups.

The decrease in collagen fiber alignment observed for T_1 in the US group is also consistent with the decrease in T_2^* times we observed. This is consistent with the study by Chu *et al.* using ultra-echo time (UTE) techniques and the finding that UTE T_2^* mapping can detect deep tissue cartilage changes (45). Moreover, previous research has demonstrated that the addition of ASC or BMSC can lead to full restoration of collagen alignment over a period of several months (46,47). The study by Seifarth *et al.* suggests that the scaffold structure may play a role in collagen alignment in unseeded collagen scaffolds (48).

Fifth and finally, $T_{1\rho}$ measurements were performed, but no significant changes were observed. In previous *in vitro* studies, $T_{1\rho}$ showed PG sensitivity (49,50). For example, collagen and PG loss in bovine articular cartilage caused by trypsin was observed in the study by Duvvuri *et al.* (49). However, the $T_{1\rho}$ time in healthy cartilage was 106 ms and prolonged to 115 ms with 70% PG loss. Compared to the other biosensitive sequences, the measurement of $T_{1\rho}$ requires a long measurement time and has low resolution. Therefore, it is possible that no biomorphological changes were observed due to partial volume effects and local degeneration. This is also in agreement with the study by van Tiel *et al.* who investigated the high specificity of $T_{1\rho}$ for GAG observed *in vitro* using dGEMRIC in an *in vivo* study and did not find it for $T_{1\rho}$ (51).

Although the findings were obtained from an *ex vivo* minipig model, our study suggests that the T_2 imaging technique may be a valuable and contrast-free alternative to the dGEMRIC technique in evaluating the regeneration potential of different treatment strategies for knee cartilage repair. We observed an increase in T_2 values within the defect region in the defect group, which might suggest an accumulation of free water such as synovial fluid. In contrast, we observed a slight but significant decrease in T_2 times in the ASC region, potentially indicating a higher GAG concentration within the defect compared to the surrounding tissue. These results imply that T_2 imaging could serve as a useful, contrast-free alternative for evaluating cartilage regeneration in future *in vivo* studies.

In our model, defects were created surgically. Compared to models in which pathologic cartilage degenerations were achieved by trypsin or complete rupture of the anterior cruciate ligament, surgical defect induction defect enables targeted and localized cartilage degeneration (43,52). Therefore, we could reference the results within a knee joint

(defect *vs.* femur and tibia), which makes the statistical test we present independent of individual differences. One of the strengths of our statistical analysis was that we were able to examine and compare the cartilage regions within one knee, so that individual differences between pigs, such as different walking or standing times, did not affect the statistics.

In regard to potential risks, side effects, and systemic implications of the treatments and MRI techniques employed, it is important to note that no systemic effects were expected due to the MSC application for several reasons: (I) it is known that MSCs have low immunogenicity; (II) autologous MSCs were applicated; (III) MSCs were applicated locally; (IV) MSC have anti-inflammatory properties; (V) in our prior studies (34,53) we have also observed neither side effects nor systemic effects. These observations align with those reported in the very good overview articles by Nitkin & Bonfield and Saeed *et al.* (54,55), who similarly did not report systemic effects with comparable treatments in a broader context of regeneration. The problem with MSC therapy tends not to be the rejection but rather a lack of efficacy (54).

Although our study was applicable to all groups and the T_2 assessment proved to be as sensitive as the dGEMRIC technique, some limitations need to be considered. First, an animal model was used in this study. Although the minipig model is considered a valid model for studying cartilage degeneration, there are differences between the minipig and the human body, especially in terms of size. Compared to humans minipigs have more chondrocytes in their cartilage, which could lead to a higher regeneration potential compared to humans (33,56). Despite this supposedly good healing potential, the study showed significant cartilage damage in the untreated defects as opposed to the treated ones, further reinforcing the importance of therapy. Second, we performed the measurement in an *ex vivo* model, so measurements at multiple time points were not possible. To better assess the regeneration potential, biosensitive MR measurements at multiple time points would be of interest, analogous to previous studies by Tsai *et al.* in a rat model (57). Due to the limited storage capabilities of minipigs in a clinical 3 Tesla MR scanner and animal ethical concerns due to the anaesthesia required, we refrained from measurements at multiple time points. Third, in routine clinical practice, dGEMRIC images are usually acquired after a 90-minute delay following injection of gadolinium contrast agent to allow for diffusion and contrast enhancement in tissue (10). In our study, specimens were collected *ex vivo*, i.e., the joint capsule was first surgically opened, and then the entire

specimen was placed in a contrast medium solution for 60 minutes. Before the specimen was stored back in the scanner, we removed the contrast medium from the joint capsule again; however, contrast medium fluid may still be present in the capsule and thus affect the readings locally. However, since we refer to each individual knee in our study, the dependence is reduced. Fourth, a limited number of animals were examined in this study. By comparing different cartilage regions within the same knee, we were able to minimize the individual influence of different pigs, so that even a smaller number of animals leads to adequate results. Fifth, this study was performed exclusively with respect to biosensitive MR sequences. However, it is also of great clinical interest to evaluate the regeneration potential in terms of various histological parameters to obtain a comprehensive assessment. Sixth, a potential limitation of our study is that we did not perform *in vivo* MRI immediately post-injury due to considerations regarding animal welfare, logistical constraints, and methodological accuracy. Future studies could potentially incorporate *in vivo* imaging at multiple time points, provided appropriate care is taken to minimize animal stress and ensure biosafety regulations are adhered to.

Conclusions

In this preclinical study, we evaluated compositional MR sequences' ability to depict the regenerative potential of knee cartilage, applying various therapies, including ASC, BMSC, US, and conservative treatment, to standardized cartilage defects. Our results emphasize the dGEMRIC technique's excellence for quantitative imaging of cartilage, but also highlight non-contrast T_2 imaging's reliability and comparable sensitivity. Consequently, T_2 imaging is a feasible, contrast-free alternative to dGEMRIC and is recommended for future research. These results were obtained from a preclinical model; thus, further validation in clinical settings is required. We also advocate for longitudinal clinical studies utilizing T_2 imaging to understand these therapies' long-term effects.

Acknowledgments

Footnote

Reporting Checklist: The authors have completed the ARRIVE reporting checklist. Available at https://qims.amegroups.com/article/view/10.21037/qims-23-570/rc

Conflicts of Interest: All authors have completed the ICMJE uniform disclosure form (available at https://qims.amegroups.com/article/view/10.21037/qims-23-570/coif). VG, PJ and JW report that the study was supported by the Deutsche Arthrose-Hilfe grant number: P460-A335-Windolf-EP2-jung1-knie-op-I-25k-2019-20. VG reports that this study was supported by collagen scaffolds from Matricel GmbH. The other authors have no conflicts of interest to declare.

Ethical Statement: The authors are accountable for all aspects of the work in ensuring that questions related to the accuracy or integrity of any part of the work are appropriately investigated and resolved. Experiments were performed in accordance with the institutional guidelines for the care and use of laboratory animals at the Heinrich Heine University, Medical Faculty. The study was approved by the regional authority: Landesamt für Natur-, Umwelt- und Verbraucherschutz, LANUV NRW, Germany under application number: 81-02.04.2020.A198.

Open Access Statement: This is an Open Access article distributed in accordance with the Creative Commons Attribution-NonCommercial-NoDerivs 4.0 International License (CC BY-NC-ND 4.0), which permits the non-commercial replication and distribution of the article with the strict proviso that no changes or edits are made and the original work is properly cited (including links to both the formal publication through the relevant DOI and the license). See: https://creativecommons.org/licenses/by-nc-nd/4.0/.

References

1. Lawrence RC, Felson DT, Helmick CG, Arnold LM, Choi H, Deyo RA, Gabriel S, Hirsch R, Hochberg MC, Hunder GG, Jordan JM, Katz JN, Kremers HM, Wolfe F; National Arthritis Data Workgroup. Estimates of the prevalence of arthritis and other rheumatic conditions in the United States. Part II. Arthritis Rheum 2008;58:26-35.

2. Bliddal H, Leeds AR, Christensen R. Osteoarthritis, obesity and weight loss: evidence, hypotheses and horizons - a scoping review. Obes Rev 2014;15:578-86.

3. Tonge DP, Pearson MJ, Jones SW. The hallmarks of osteoarthritis and the potential to develop personalised disease-modifying pharmacological therapeutics. Osteoarthritis Cartilage 2014;22:609-21.

4. Abrar DB, Schleich C, Radke KL, Frenken M, Stabinska J, Ljimani A, Wittsack HJ, Antoch G, Bittersohl B, Hesper T, Nebelung S, Müller-Lutz A. Detection of early cartilage degeneration in the tibiotalar joint using 3 T gagCEST imaging: a feasibility study. MAGMA 2021;34:249-60.

5. Leonhäuser D, Stollenwerk K, Seifarth V, Zraik IM, Vogt M, Srinivasan PK, Tolba RH, Grosse JO. Two differentially structured collagen scaffolds for potential urinary bladder augmentation: proof of concept study in a Göttingen minipig model. J Transl Med 2017;15:3.

6. Rubessa M, Polkoff K, Bionaz M, Monaco E, Milner DJ, Holllister SJ, Goldwasser MS, Wheeler MB. Use of Pig as a Model for Mesenchymal Stem Cell Therapies for Bone Regeneration. Anim Biotechnol 2017;28:275-87.

7. Ruetze M, Richter W. Adipose-derived stromal cells for osteoarticular repair: trophic function versus stem cell activity. Expert Rev Mol Med 2014;16:e9.

8. Abrar DB, Schleich C, Nebelung S, Frenken M, Ullrich T, Radke KL, Antoch G, Vordenbäumen S, Brinks R, Schneider M, Ostendorf B, Sewerin P. Proteoglycan loss in the articular cartilage is associated with severity of joint inflammation in psoriatic arthritis-a compositional magnetic resonance imaging study. Arthritis Res Ther 2020;22:124.

9. Dunn TC, Lu Y, Jin H, Ries MD, Majumdar S. T2 relaxation time of cartilage at MR imaging: comparison with severity of knee osteoarthritis. Radiology 2004;232:592-8.

10. Guermazi A, Alizai H, Crema MD, Trattnig S, Regatte RR, Roemer FW. Compositional MRI techniques for evaluation of cartilage degeneration in osteoarthritis. Osteoarthritis Cartilage 2015;23:1639-53.

11. Truhn D, Zwingenberger KT, Schock J, Abrar DB, Radke KL, Post M, Linka K, Knobe M, Kuhl C, Nebelung S. No pressure, no diamonds? - Static vs. dynamic compressive in-situ loading to evaluate human articular cartilage functionality by functional MRI. J Mech Behav Biomed Mater 2021;120:104558.

12. Radke KL, Abrar DB, Frenken M, Wilms LM, Kamp B, Boschheidgen M, Liebig P, Ljimani A, Filler TJ, Antoch G, Nebelung S, Wittsack HJ, Müller-Lutz A. Chemical Exchange Saturation Transfer for Lactate-Weighted Imaging at 3 T MRI: Comprehensive In Silico, In Vitro, In Situ, and In Vivo Evaluations. Tomography 2022;8:1277-92.

13. Radke KL, Wilms LM, Frenken M, Stabinska J, Knet M, Kamp B, Thiel TA, Filler TJ, Nebelung S, Antoch G, Abrar DB, Wittsack HJ, Müller-Lutz A. Lorentzian-Corrected Apparent Exchange-Dependent Relaxation (LAREX) Ω-Plot Analysis-An Adaptation for qCEST in a Multi-Pool System: Comprehensive In Silico, In Situ, and In Vivo Studies. Int J Mol Sci 2022;23:6920.

14. Bechler E, Stabinska J, Thiel T, Jasse J, Zukovs R, Valentin B, Wittsack HJ, Ljimani A. Feasibility of quantitative susceptibility mapping (QSM) of the human kidney. MAGMA 2021;34:389-97.

15. Kamp B, Frenken M, Klein-Schmeink L, Nagel AM, Wilms LM, Radke KL, Tsiami S, Sewerin P, Baraliakos X, Antoch G, Abrar DB, Wittsack HJ, Müller-Lutz A. Evaluation of Sodium Relaxation Times and Concentrations in the Achilles Tendon Using MRI. Int J Mol Sci 2022;23:10890.

16. Matzat SJ, van Tiel J, Gold GE, Oei EH. Quantitative MRI techniques of cartilage composition. Quant Imaging Med Surg 2013;3:162-74.

17. Li X, Benjamin Ma C, Link TM, Castillo DD, Blumenkrantz G, Lozano J, Carballido-Gamio J, Ries M, Majumdar S. In vivo T(1rho) and T(2) mapping of articular cartilage in osteoarthritis of the knee using 3 T MRI. Osteoarthritis Cartilage 2007;15:789-97.

18. Buckwalter JA. Articular cartilage: composition and structure. Injury and Repair of the Musculoskeletal Soft Tissues. 1991.

19. Burstein D, Gray M, Mosher T, Dardzinski B. Measures of molecular composition and structure in osteoarthritis. Radiol Clin North Am 2009;47:675-86.

20. Bashir A, Gray ML, Burstein D. Gd-DTPA2- as a measure of cartilage degradation. Magn Reson Med 1996;36:665-73.

21. 21. Burstein D, Velyvis J, Scott KT, Stock KW, Kim YJ, Jaramillo D, Boutin RD, Gray ML. Protocol issues for delayed Gd(DTPA)(2-)-enhanced MRI (dGEMRIC) for clinical evaluation of articular cartilage. Magn Reson Med 2001;45:36-41.

22. Wang L, Regatte RR. T$_1\rho$ MRI of human musculoskeletal system. J Magn Reson Imaging 2015;41:586-600.

23. Akella SV, Regatte RR, Gougoutas AJ, Borthakur A, Shapiro EM, Kneeland JB, Leigh JS, Reddy R. Proteoglycan-induced changes in T1rho-relaxation of articular cartilage at 4T. Magn Reson Med 2001;46:419-23.

24. Rauscher I, Bender B, Grözinger G, Luz O, Pohmann R, Erb M, Schick F, Martirosian P. Assessment of T1, T1 , and T2 values of the ulnocarpal disc in healthy subjects at 3 tesla. Magn Reson Imaging 2014;32:1085-90.

25. Raaphorst GP, Law P, Kruuv J. Water content and spin lattice relaxation times of cultured mammalian cells subjected to various salt, sucrose, or DMSO solutions. Physiol Chem Phys 1978;10:177-191.

26. Marinelli NL, Haughton VM, Muñoz A, Anderson PA. T2 relaxation times of intervertebral disc tissue correlated with water content and proteoglycan content. Spine (Phila Pa 1976) 2009;34:520-4.

27. Beveridge JE, Machan JT, Walsh EG, Kiapour AM, Karamchedu NP, Chin KE, Proffen BL, Sieker JT, Murray MM, Fleming BC. Magnetic resonance measurements of tissue quantity and quality using T(2) * relaxometry predict temporal changes in the biomechanical properties of the healing ACL. J Orthop Res 2018;36:1701-9.

28. Wilms LM, Radke KL, Latz D, Thiel TA, Frenken M, Kamp B, Filler TJ, Nagel AM, Müller-Lutz A, Abrar DB, Nebelung S. UTE-T2* versus conventional T2* mapping to assess posterior cruciate ligament ultrastructure and integrity-an in-situ study. Quant Imaging Med Surg 2022;12:4190-201.

29. Giannasi C, Niada S, Magagnotti C, Ragni E, Andolfo A, Brini AT. Comparison of two ASC-derived therapeutics in an in vitro OA model: secretome versus extracellular vesicles. Stem Cell Res Ther 2020;11:521.

30. Ye Y, Peng YR, Hu SQ, Yan XL, Chen J, Xu T. In Vitro Differentiation of Bone Marrow Mesenchymal Stem Cells into Neuron-Like Cells by Cerebrospinal Fluid Improves Motor Function of Middle Cerebral Artery Occlusion Rats. Front Neurol 2016;7:183.

31. Horbert V, Xin L, Föhr P, Huber R, Burgkart RH, Kinne RW. In Vitro Cartilage Regeneration with a Three-Dimensional Polyglycolic Acid (PGA) Implant in a Bovine Cartilage Punch Model. Int J Mol Sci 2021.

32. Pearce AI, Richards RG, Milz S, Schneider E, Pearce SG. Animal models for implant biomaterial research in bone: a review. Eur Cell Mater 2007;13:1-10.

33. Gotterbarm T, Breusch SJ, Schneider U, Jung M. The minipig model for experimental chondral and osteochondral defect repair in tissue engineering: retrospective analysis of 180 defects. Lab Anim 2008;42:71-82.

34. Betsch M, Thelen S, Santak L, Herten M, Jungbluth

P, Miersch D, Hakimi M, Wild M. The role of erythropoietin and bone marrow concentrate in the treatment of osteochondral defects in mini-pigs. PLoS One 2014;9:e92766.

35. Möllers S, Heschel I, Damink LH, Schügner F, Deumens R, Müller B, Bozkurt A, Nava JG, Noth J, Brook GA. Cytocompatibility of a novel, longitudinally microstructured collagen scaffold intended for nerve tissue repair. Tissue Eng Part A 2009;15:461-72.

36. Jurgens WJ, Kroeze RJ, Bank RA, Ritt MJ, Helder MN. Rapid attachment of adipose stromal cells on resorbable polymeric scaffolds facilitates the one-step surgical procedure for cartilage and bone tissue engineering purposes. J Orthop Res 2011;29:853-60.

37. Freedman JD, Ellis DJ, Lusic H, Varma G, Grant AK, Lakin BA, Snyder BD, Grinstaff MW. dGEMRIC and CECT Comparison of Cationic and Anionic Contrast Agents in Cadaveric Human Metacarpal Cartilage. J Orthop Res 2020;38:719-25.

38. Stewart RC, Bansal PN, Entezari V, Lusic H, Nazarian RM, Snyder BD, Grinstaff MW. Contrast-enhanced CT with a high-affinity cationic contrast agent for imaging ex vivo bovine, intact ex vivo rabbit, and in vivo rabbit cartilage. Radiology 2013;266:141-50.

39. Bashir A, Gray ML, Boutin RD, Burstein D. Glycosaminoglycan in articular cartilage: in vivo assessment with delayed Gd(DTPA)(2-)-enhanced MR imaging. Radiology 1997;205:551-8.

40. Allen RG, Burstein D, Gray ML. Monitoring glycosaminoglycan replenishment in cartilage explants with gadolinium-enhanced magnetic resonance imaging. J Orthop Res 1999;17:430-6.

41. Owman H, Ericsson YB, Englund M, Tiderius CJ, Tjörnstrand J, Roos EM, Dahlberg LE. Association between delayed gadolinium-enhanced MRI of cartilage (dGEMRIC) and joint space narrowing and osteophytes: a cohort study in patients with partial meniscectomy with 11 years of follow-up. Osteoarthritis Cartilage 2014;22:1537-41.

42. David-Vaudey E, Ghosh S, Ries M, Majumdar S. T2 relaxation time measurements in osteoarthritis. Magn Reson Imaging 2004;22:673-82.

43. Wei B, Zong M, Yan C, Mao F, Guo Y, Yao Q, Xu Y, Wang L. Use of quantitative MRI for the detection of progressive cartilage degeneration in a mini-pig model of osteoarthritis caused by anterior cruciate ligament transection. J Magn Reson Imaging 2015;42:1032-8.

44. Tiderius CJ, Olsson LE, Leander P, Ekberg O, Dahlberg L. Delayed gadolinium-enhanced MRI of cartilage (dGEMRIC) in early knee osteoarthritis. Magn Reson Med 2003;49:488-92.

45. Chu CR, Williams AA, West RV, Qian Y, Fu FH, Do BH, Bruno S. Quantitative Magnetic Resonance Imaging UTE-T2* Mapping of Cartilage and Meniscus Healing After Anatomic Anterior Cruciate Ligament Reconstruction. Am J Sports Med 2014;42:1847-56.

46. Lazarini M, Bordeaux-Rego P, Giardini-Rosa R, Duarte ASS, Baratti MO, Zorzi AR, de Miranda JB, Lenz Cesar C, Luzo Â, Olalla Saad ST. Natural Type II Collagen Hydrogel, Fibrin Sealant, and Adipose-Derived Stem Cells as a Promising Combination for Articular Cartilage Repair. Cartilage 2017;8:439-43.

47. Lv X, He J, Zhang X, Luo X, He N, Sun Z, Xia H, Liu V, Zhang L, Lin X, Lin L, Yin H, Jiang D, Cao W, Wang R, Zhou G, Wang W. Comparative Efficacy of Autologous Stromal Vascular Fraction and Autologous Adipose-Derived Mesenchymal Stem Cells Combined With Hyaluronic Acid for the Treatment of Sheep Osteoarthritis. Cell Transplant 2018;27:1111-25.

48. Seifarth V, Gossmann M, Janke HP, Grosse JO, Becker C, Heschel I, Artmann GM, Temiz Artmann A. Development of a Bioreactor to Culture Tissue Engineered Ureters Based on the Application of Tubular OPTIMAIX 3D Scaffolds. Urol Int 2015;95:106-13.

49. Duvvuri U, Kudchodkar S, Reddy R, Leigh JS. T(1rho) relaxation can assess longitudinal proteoglycan loss from articular cartilage in vitro. Osteoarthritis Cartilage 2002;10:838-44.

50. Hatcher CC, Collins AT, Kim SY, Michel LC, Mostertz WC 3rd, Ziemian SN, Spritzer CE, Guilak F, DeFrate LE, McNulty AL. Relationship between T1rho magnetic resonance imaging, synovial fluid biomarkers, and the biochemical and biomechanical properties of cartilage. J Biomech 2017;55:18-26.

51. van Tiel J, Kotek G, Reijman M, Bos PK, Bron EE, Klein S, Nasserinejad K, van Osch GJ, Verhaar JA, Krestin GP, Weinans H, Oei EH. Is T1ρ Mapping an Alternative to Delayed Gadolinium-enhanced MR Imaging of Cartilage in the Assessment of Sulphated Glycosaminoglycan Content in Human Osteoarthritic Knees? An in Vivo Validation Study. Radiology 2016;279:523-31.

52. Hafner T, Schock J, Post M, Abrar DB, Sewerin P, Linka K, Knobe M, Kuhl C, Truhn D, Nebelung S. A serial multiparametric quantitative magnetic resonance imaging study to assess proteoglycan depletion of human articular cartilage and its effects on functionality. Sci Rep

2020;10:15106.

53. Jungbluth P, Spitzhorn LS, Grassmann J, Tanner S, Latz D, Rahman MS, Bohndorf M, Wruck W, Sager M, Grotheer V, Kröpil P, Hakimi M, Windolf J, Schneppendahl J, Adjaye J. Human iPSC-derived iMSCs improve bone regeneration in mini-pigs. Bone Res 2019;7:32.

54. Nitkin CR, Bonfield TL. Concise Review: Mesenchymal Stem Cell Therapy for Pediatric Disease: Perspectives on Success and Potential Improvements. Stem Cells Transl Med 2017;6:539-65.

55. Saeed H, Ahsan M, Saleem Z, Iqtedar M, Islam M, Danish Z, Khan AM. Mesenchymal stem cells (MSCs) as skeletal

therapeutics - an update. J Biomed Sci 2016;23:41.

56. Ha CW, Park YB, Chung JY, Park YG. Cartilage Repair Using Composites of Human Umbilical Cord Blood-Derived Mesenchymal Stem Cells and Hyaluronic Acid Hydrogel in a Minipig Model. Stem Cells Transl Med 2015;4:1044-51.

57. Tsai PH, Lee HS, Siow TY, Chang YC, Chou MC, Lin MH, Lin CY, Chung HW, Huang GS. Sequential change in T2* values of cartilage, meniscus, and subchondral bone marrow in a rat model of knee osteoarthritis. PLoS One 2013;8:e76658.